A heuristic approach to the infinite-ranged spin-glass model

1989 J. Phys. A: Math. Gen. 22 93

(http://iopscience.iop.org/0305-4470/22/1/016)

J. Phys. A: Math. Gen. **22** (1989) 93-103. Printed in the UK

A heuristic approach to the infinite-ranged spin-glass model

Kazuo Nokura

Department of Physics, Kyoto University, Kyoto 606, Japan

Received 15 March 1988, in final form 1 August 1988

Abstract. The local minima of the Sherrington-Kirkpatrick model are studied numerically by introducing a heuristic method. Our approach naturally leads us to their ultrametricity. For finite systems some observations on this method suggest the relation $d_1 - d_2 \sim \sqrt{d_3}$ among three distances of three low-energy local minima $d_1 \geqslant d_2 \geqslant d_3$. Overlap functions are studied numerically, giving consistent results with the above relation and the results of the replica symmetry breaking theory.

1. Introduction

One of the main interests in the spin-glass phase is in the expectation that it can be a disordered system of a new type of magnetic order which cannot be reduced to ordinary ferromagnetism. In particular, many studies suggest that it is characterised primarily by a large number of deep free-energy valleys. Among them, the replica symmetry breaking solution [1] of the Sherrington-Kirkpatrick (SK) model [2] presents us with precise ideas on this problem [3]. In addition to ordinary thermodynamics, this solution presents us with two novel aspects of the spin-glass phase, which are well described by a new type of order parameter called the overlap function [4]. The first is that natural distances between these valleys are sample dependent even in the thermodynamic limit. The second is that these valleys are organised in a hierarchy which is characterised by an ultrametric structure. That is, the three distances of any set of three valleys form a triangle which is either equilateral or isosceles with the third edge shortest. Some numerical efforts to check these results have been presented by several authors [5-7]. It has also been suggested that these properties are universal [8]. In this paper, in order to add another point of view which will hopefully clarify the origin of this structure, we shall introduce a heuristic method to obtain a large number of local minima of the SK model. The point of this method is based on the idea that $P(h)$, the distribution of the effective field over the system, reflects the organisation of the low-energy local minima ($T = 0$ valleys). This idea was inspired by the study of a simple infinite-ranged model [9]. In this model, by the effect of inter-subsystem frustrations, low-energy local minima are made up from independent rigid clusters of widely differing sizes. Since interactions are infinite ranged, each site of a given cluster feels the effective field proportional to the size of this cluster. In § 2, which is primarily a résumé of the previous paper [10], we study the application of this observation to the SK model and discuss the main features of the method introduced. We shall show that ultrametricity is a natural conclusion from our point of view. In § 3, in contrast to § 2, we shall regard our method simply as a way of obtaining a large number of

0305-4470/89/010093+11$02.50

local minima and we shall then study the overlap functions constructed from them. Section 4 is devoted to some discussions, especially on the short-range model.

2. A heuristic method

The Ising SK model is the infinite-ranged random Ising model, which is described by

$$H = -\sum J_{ij}\sigma_i\sigma_j \tag{1}$$

where J_{ij} are quenched random interactions which obey a Gaussian distribution with width $N^{-1/2}$ for a system of N sites. We consider the temperature $T=0$. At a local minimum, spins σ_i should satisfy the stability conditions

$$\sigma_i h_i > 0 \tag{2}$$

$$h_i = \sum_{j\neq i} J_{ij}\sigma_j \tag{3}$$

for all i, where h_i is the effective field on the site i. Starting from random configurations these states are easily obtained by iterations of spin flip, which always makes the energy lower (the one-spin-flip method). The properties of overlap functions below $T_C=1$ are characterised by the states α with $E_\alpha - E_0 \sim O(1)$, where E_α is the energy of the state α and E_0 is the energy of the lowest state. It is rather difficult to obtain these low-energy local minima by this method, especially for large N. To introduce our method we first study the distribution of the effective field over the system which is defined by

$$P(h) = \frac{1}{N}\sum_{i=1}^{N}\delta(h_i - h). \tag{4}$$

At an early stage in the study of the SK model, Anderson pointed out that $P(h)$ is proportional to $|h|$ for small $|h|$ [11]. This property was also affirmed numerically [12]. Since this property is crucial in our approach, we reproduce the argument presented by him. For a given local minimum it is suggested that we consider the cluster of sites with the effective field smaller than h $(0<h\ll 1)$, which we denote by $S_h=\{i||h_i|<h\}$. The number of sites which belong to S_h is given by $n=|S_h|=2N\int_0^h P(h)\,\mathrm{d}h$. The whole system is divided into two regions, S_h and $\bar{S}_h$, where $\bar{S}_h$ is the complement of S_h. Let us introduce two effective fields given by

$$h_i^{\mathrm{I}} = \sum_{j\in S_h} J_{ij}\sigma_j \tag{5}$$

$$h_i^{\mathrm{E}} = \sum_{j\in \bar{S}_h} J_{ij}\sigma_j. \tag{6}$$

If $i\in S_h$, h_i^{I} is the effective field produced by S_h itself, and estimated to be $(n/N)^{1/2}$. Then, by demanding the consistency $h\sim h_i^{\mathrm{I}}$, we reach the relation $P(h)\propto|h|$. This argument further implies that $h_i^{\mathrm{E}}\sim h$, since $h_i = h_i^{\mathrm{I}} + h_i^{\mathrm{E}} \sim h$. This means that the effective field on S_h produced by $\bar{S}_h$ is rather small, despite the large number of spins in $\bar{S}_h$. This situation is very similar to the model with inter-subsystem frustration [9]. Hence it is natural to study cooperative spin flips in S_h to search other low-energy local minima. Let us consider what happens to this state α if we set $\sigma_i \to -\sigma_i$ for all $i\in S_h$. It is easily shown that the stability conditions are violated by this operation. The

degree of this violation can be estimated in the following way. With this operation, $C_j = h_j\sigma_j$ is replaced by

$$C_j' = (h_j^{\mathrm{I}} - h_j^{\mathrm{E}})\sigma_j \tag{7}$$

for all $j \in S_h$. We see that C_j' is either positive or negative with probability $\frac{1}{2}$ if we notice $\langle |h_i^{\mathrm{I}}| \rangle_s \sim \langle |h_i^{\mathrm{E}}| \rangle_s$, where $\langle\ \rangle_s$ means the site average over S_h. For $j \in \bar{S}_h$, we have $C_j' = (h_j^{\mathrm{E}} - h_j^{\mathrm{I}})\sigma_j$, which remains positive for the site with $h_j\sigma_j \gg h$. We then expect that if we apply the one-spin-flip method to this state we will have another local minimum, β, in which spin flips take place for the sites with $|h_i| \lesssim h$. We introduce $R_h = \{i | \sigma_i^\alpha \sigma_i^\beta = -1\}$. Figures 1 and 2 show the typical numerical results. In figure 1, with $h = 0.1n$ $(n = 1, 2, \ldots, 20)$, the relation between $|S_h|$ and $|R_h|$ is presented for five starting states of a sample. In figure 2, the relation between $|S_h|$ and $|R_h \cap \bar{S}_h|$ are presented for the same sequences. We should note that $|R_h \cap \bar{S}_h|$ is much smaller than $|R_h|$, and $|R_h|$ is nearly equal to $|S_h|/2$ at $|S_h| \sim 20$, 50 and 100 for some sequences. These results imply that, at these points, about half of the spins remain to be flipped with little change in $\bar{S}_h$. These numbers presumably reflect the structure of the configuration space. Unfortunately we have no argument to affirm that $\Delta E = E_\alpha - E_\beta \sim O(1)$. The computer calculations show that ΔE depends upon many factors, e.g. sample, starting state and h. However, we usually obtained states with energy nearly equal to or lower than the energy of original starting states for small h. This point depends upon the energy of the starting states and will be discussed in the next section.

We can regard our method just as a way of obtaining a large number of local minima. We shall take this point of view in the next section. Here we want to point

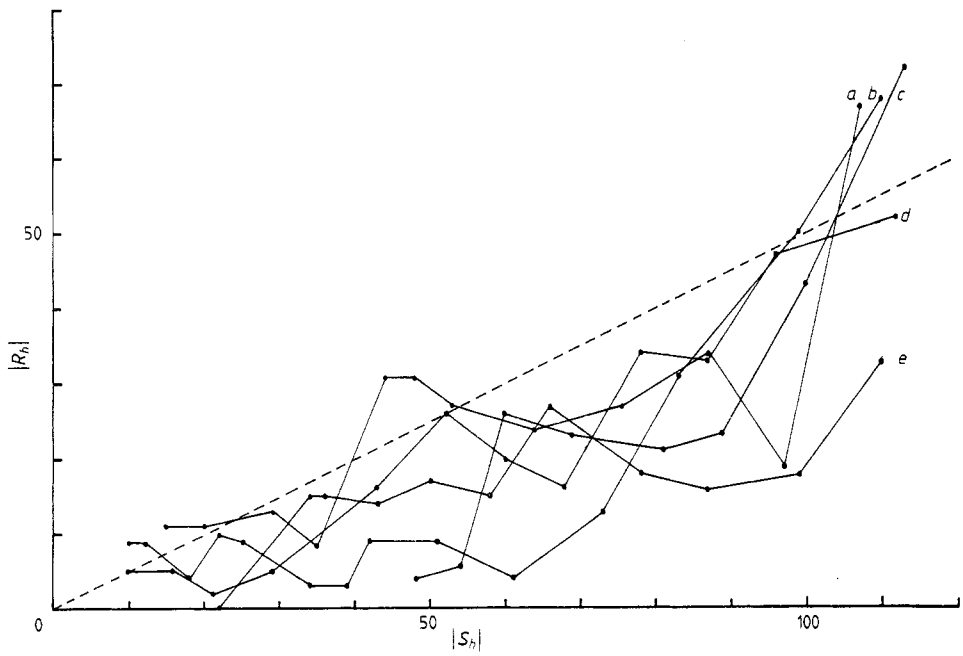

Figure 1. Some examples of the relation between $|R_h|$ and $|S_h|$. This picture is depicted for one sample of $N = 200$ and five starting states. The points on each zigzag line represent the $|S_h| - |R_h|$ relation for one starting state with $h = 0.1n$ $(n = 1, \ldots, 20)$. The details around $|R_h| \sim 0$ are omitted to avoid complexity. The broken line is $|R_h| = |S_h|/2$.

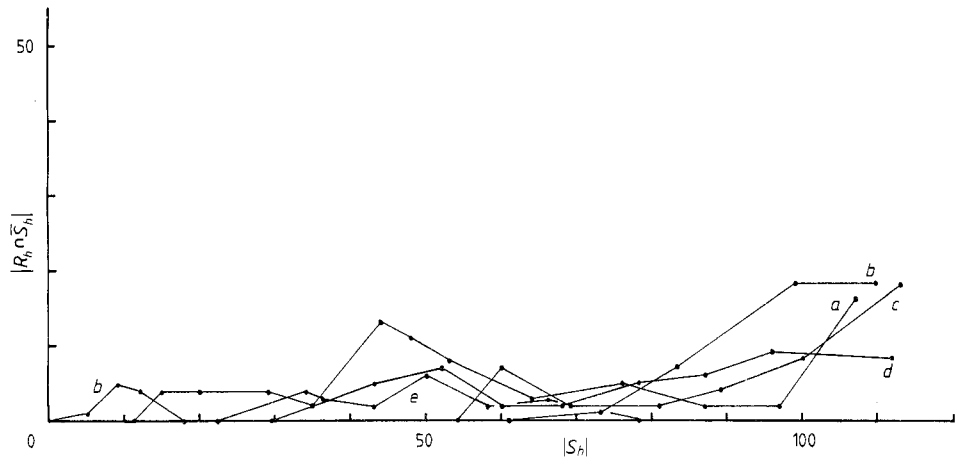

Figure 2. The relations between $|R_h|$ and $|R_h \cap \bar{S}_h|$ for the same sequences of figure 1. Some isolated short lines with $|R_h \cap \bar{S}_h| \leq 4$, one of which is shown for *b*, are omitted for *c*, *d* and *e*.

out that figures 1 and 2 give a fruitful insight into the structure of local minima. Let us consider the relation between $R_{h\beta}$ and $R_{h\gamma}$ which, from α, are obtained by our method with $h_\gamma \gg h_\beta$. We consider the maximal situation $|R_h| \sim |S_h|/2$, which means that a site in S_h belongs to R_h with probability $\frac{1}{2}$. The relation between $R_{h\gamma}$ and $R_{h\beta}$ has any possibility among $0 \leq |R_{h\gamma} \cap R_{h\beta}| \leq |R_{h\beta}|$. Here we suggest that the spin flips in $S_{h\gamma}$ and $S_{h\beta}$ have no correlation, since the set of interactions J_{ij} with $i \in S_h$ and $j \in \bar{S}_h$, which control the spin flips in S_h, has different random variables for each h. With this assumption a site in $R_{h\beta}$, which belongs to $S_{h\gamma}$, also belongs to $R_{h\gamma}$ with probability $\frac{1}{2}$. We then have $|R_{h\beta} \cap R_{h\gamma}| = \frac{1}{2}|R_{h\beta}| + O(|R_{h\beta}|^{1/2})$ for $|R_{h\gamma}| \gg |R_{h\beta}| \gg 1$. The $|R_{h\beta}|^{1/2}$ correction is due to the central limit theorem. The reason why we present these arguments is that the above relation is in agreement with the ultrametricity of local minima. That is, by using the definition of distance, $d_{\alpha\beta} = |R_{h\beta}|$, $d_{\alpha\gamma} = |R_{h\gamma}$ and $d_{\beta\gamma} = |R_{h\beta}| + |R_{h\gamma}| - 2|R_{h\beta} \cap R_{h\gamma}|$, we have $d_{\alpha\gamma} = d_{\beta\gamma} > d_{\alpha\beta}$ for large $|R_{h\beta}|$. For the finite system these arguments imply that, when three distances are arranged in the order $d_1 \geq d_2 \geq d_3$, we expect the relation $d_1 - d_2 \sim \sqrt{d_3}$. If the picture presented in this section is correct, this relation will be observed in the overlap functions of the finite system. This point will be studied in the next section.

3. Numerical results

This section is devoted to describing the results obtained by the method introduced in § 2. As promised there, we shall regard our method as just a way of searching effectively for local minima. We first explain the details of our calculations for $N = 100$, 200 and then study the overlap functions constructed from the obtained states. In the application of our method it is necessary to avoid the artificial correlations among the resulted states. Thus we chose ten low-energy states obtained from K random configuration by the one-spin-flip method ($K = 100$, 2000 for $N = 100$, 200) and then apply our method to each of them with $h = 0.1n$ ($n = 1, 2, \ldots, 20$). The number ten is the order of the number of the states obtained which satisfy the condition $E_\alpha - E_0 \sim O(1)$.

We take 21 and 10 samples for both $N = 100, 200$. To see how this method works, we also studied a few $N = 100$ samples by the one-spin-flip method with many initial random configurations. It is worthwhile to mention that, at least for $N = 100$, the one-spin-flip method gives the lowest state many times, yet slightly higher states with $E_\alpha - E_0 \sim O(1)$ appear few times in comparison with our method. For $N = 200$, the lowest state rarely exists in the ten starting states and our method usually finds lower states close to the original starting state. In achieving a local minimum from the configuration obtained by $\sigma_i \to -\sigma_i$ for $i \in S_h$, we tried several options of the one-spin-flip method which have a different order of spin flips. For $N = 200$, four options seem to be sufficient to obtain the possible states with $E_\alpha - E_0 \sim O(1)$. The lowest energy $\langle E_0 \rangle / N$ was found to be -0.7407 for $N = 100$ and -0.7440 for $N = 200$, where $\langle\ \rangle$ means the sample average. The number n_l of the obtained local minima with $E_\alpha - E_0 \leqslant 1$ strongly depends upon samples. We found $1 \leqslant n_l \leqslant 14$ with $\langle n_l \rangle = 7.3$ for $N = 100$ and $7 \leqslant n_l \leqslant 40$ with $\langle n_l \rangle = 23$ for $N = 200$. The value for $N = 100$ seems smaller than the value in [12]. These numbers, however, only give us a rough idea of n_l, and will be modified a little if we add other samples.

Having local minima for each sample, we can construct the overlap functions which are defined by

$$P_2(d) = \sum_{\alpha\beta} P_\alpha P_\beta \delta(d_{\alpha\beta} - d) \tag{8}$$

$$P_3(d_1, d_2, d_3) = \sum_{\alpha\beta\gamma} P_\alpha P_\beta P_\gamma \delta(d_{\alpha\beta} - d_1)\delta(d_{\beta\gamma} - d_2)\delta(d_{\alpha\gamma} - d_3) \tag{9}$$

where $P_\alpha = \exp(-\beta E_\alpha)/Z$, $Z = \Sigma_\alpha \exp(-\beta E_\alpha)$ and $\beta = T^{-1}$. Instead of the overlap $q_{\alpha\beta} = \Sigma_i \sigma_i^\alpha \sigma_i^\beta / N$, we use the distance $d_{\alpha\beta}$ which is the number of spin flips necessary to reach β from α. They have the relation $d_{\alpha\beta} = N(1 - q_{\alpha\beta})/2$. Since the number in our sample is not large, we shall study d averaged with overlap functions instead of $P_2(d)$ and $P_3(d_1, d_2, d_3)$ themselves. We first study the average $\bar{d}$ defined by

$$\bar{d} = \sum_{d=0}^{N/2} d P_2(d). \tag{10}$$

In figure 3, the temperature dependence of $\langle \bar{d} \rangle$ is presented. We study the region greater than 0.1, since the smallest value of $E_\alpha - E_0$ is of order 0.1 for almost all of the samples studied. For $T \leqslant 1$, the relation $2\langle \bar{d} \rangle / N = T$ is expected, since the susceptibility $\chi = \beta(1 - \langle \bar{q} \rangle)$ is shown to be 1 by the argument of the replica theory [1]. Figure 3 shows that $2\langle \bar{d} \rangle / N$ has a tendency to become proportional to T for large N. The deviation from T for $T \geqslant 0.3$ implies that, because of the absence of thermal fluctuations, local minima become poor approximations of free-energy valleys. We also study the root mean square $\Delta d_N = (\langle \bar{d}^2 \rangle - \langle \bar{d} \rangle^2)^{1/2}$, which characterises the sample dependence of $\bar{d}$. Figure 4 shows the temperature dependence of Δd_N. For $T < 0.15$, Δd_{200} strongly decreases as temperature is lowered. This behaviour implies that our ensemble does not have a large enough number of samples which have local minima with $E_\alpha - E_0 \leqslant 0.15$ and $d_{\alpha 0} \sim N$. We are especially interested in the N dependence of Δd_N. In figure 5, the ratio $r = \Delta d_{200} / \Delta d_{100}$ is plotted against T. In the region $0.25 < T < 0.35$, r is equal to $1.95 \approx 2.0$, which implies that Δd_N is proportional to N. This is consistent with the result $\langle P_2(d) P_2(d') \rangle \neq \langle P_2(d) \rangle \langle P_2(d') \rangle$ of the replica theory [3]. It is worthwhile pointing out the reason for the relation $\Delta d_N \propto N$ in terms of the original data. In each sample $\bar{d}$ is not determined by the average of many distances but by a few typical distances which are quite different from sample to sample. This difference is of order N, which

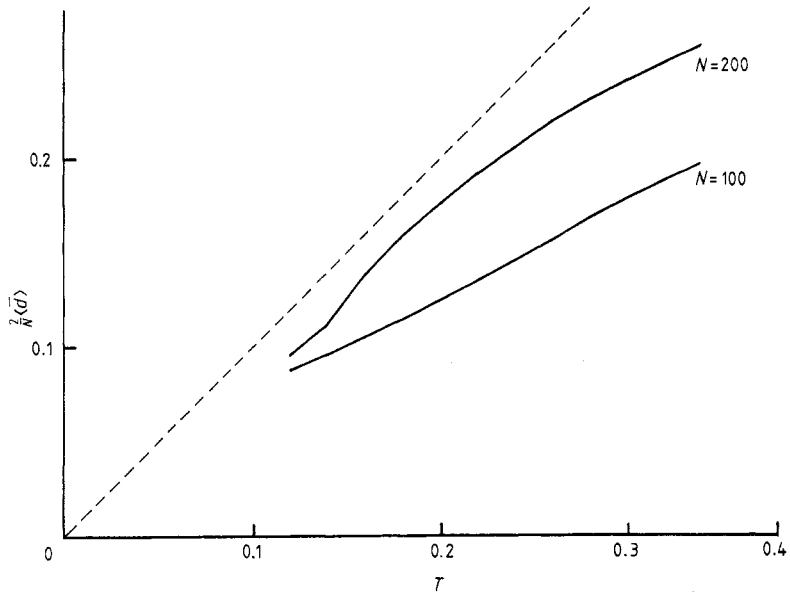

Figure 3. The temperature dependence of $2\langle\bar{d}\rangle/N$ for $N=100$ and 200. At $T=0.3$, for example, $\langle\bar{d}\rangle$ is 8.94 for $N=100$ and 24.18 for $N=200$. They provide us with an idea for the typical distances at $T=0.3$. The broken line is $2\langle\bar{d}\rangle/N=T$.

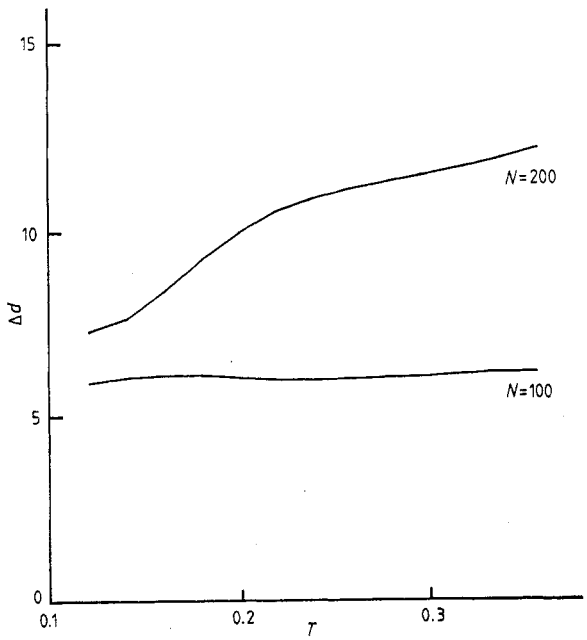

Figure 4. The temperature dependence of Δd_N.

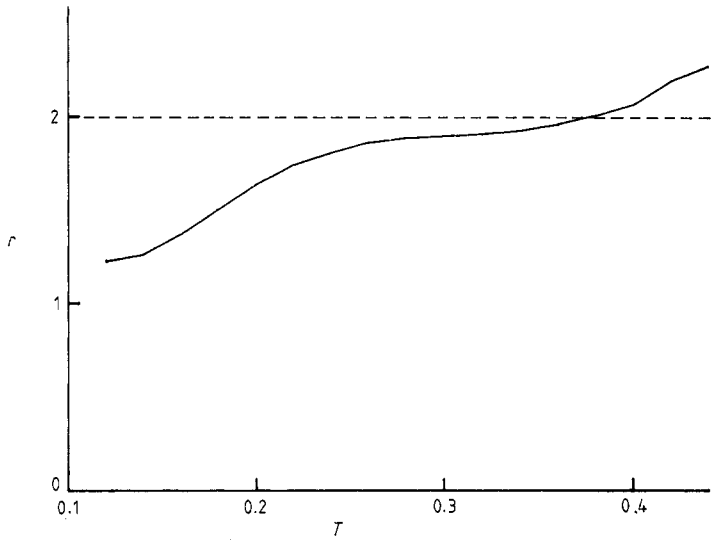

Figure 5. The temperature dependence of $r = \Delta d_{200}/\Delta d_{100}$. The broken line is $r = 2$.

leads us to the relation $\Delta d_N \propto N$. Now let us study $P_3(d_1, d_2, d_3)$. We fix the temperature at 0.3, where Δd_N shows a reasonable N dependence. As in the case of $P_2(d)$, we introduce the averages of d_i determined by $P_3(d_1, d_2, d_3)$. We restrict ourselves to the region $d_1 \geqslant d_2 \geqslant d_3$, since this function is symmetric with the permutation of d_i. Under this condition, we are first of all interested in the d_3 dependence of the difference $d_1 - d_2$. Thus we introduce the following averages:

$$\bar{d}_+(d_3) = \sum{}' (d_1 + d_2) P_3(d_1, d_2, d_3)/W(d_3) \tag{11}$$

$$\bar{d}_-(d_3) = \sum{}' (d_1 - d_2) P_3(d_1, d_2, d_3)/W(d_3) \tag{12}$$

for non-zero $W(d_3)$, where $W(d_3)$ is defined by

$$W(d_3) = \sum{}' P_3(d_1, d_2, d_3) \tag{13}$$

and Σ' means summation under the conditions $N/2 \geqslant d_1 \geqslant d_2 \geqslant d_3$ with fixed d_3. We also introduce the average of d_3 given by

$$\bar{d}_3 = \sum_{d_3=0}^{N/2} d_3 W(d_3). \tag{14}$$

$\bar{d}_\pm(1)$ is always zero, since the distance one is impossible. We are especially interested in the following two questions in terms of $\bar{d}_\pm(d_3)$ and $\bar{d}_3$. (i) Is $\bar{d}_-(d_3)$ proportional to $\sqrt{d_3}$? (ii) Are $\bar{d}_3$ and $\bar{d}_+(d_3)$ proportional to N? If these two points are confirmed, we expect the ultrametricity of local minima in the thermodynamic limit. Figure 6 shows the d_3 dependence of $\langle \bar{d}_-(d_3) \rangle$, which shows the expected behaviour for small d_3. Deviations from $\sqrt{d_3}$ take place for large d_3. We should notice here that at $T = 0.3$ the average $\langle \bar{d} \rangle$ is $8.94 \sim 9$ for $N = 100$ and $24.18 \sim 24$ for $N = 200$, as was presented in figure 3. This means that $P_3(d_1, d_2, d_3)$ for $d_i > \langle \bar{d} \rangle$ is quite small, which may cause a large deviation of $\langle \bar{d}_-(d_3) \rangle$ from the $\sqrt{d_3}$ behaviour. Thus we should restrict ourselves to the region $d_3 \leqslant \langle \bar{d} \rangle$ to study the averages introduced above. In this region $\bar{d}_-(d_3)$ has little sample dependence except for small fluctuations around $\sqrt{d_3}$. On the other hand, $\bar{d}_+(d_3)$ and $W(d_3)$ show strong sample dependences which directly reflect the

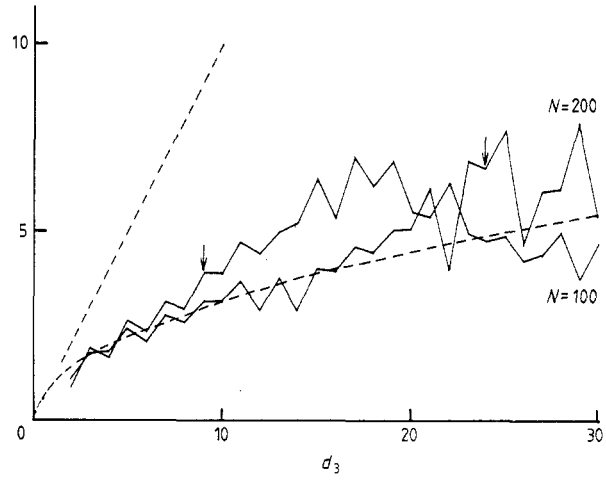

Figure 6. The d_3 dependence of $\langle \bar{d}_-(d_3) \rangle$ at $T = 0.3$. $\langle \bar{d} \rangle$ is marked by arrows for each N. The broken curve is $\sqrt{d_3}$. The broken line is d_3, which is the upper bound of $\langle \bar{d}_-(d_3) \rangle$ imposed by the triangle inequality.

dependence of $\bar{d}$. Figure 7 shows the d_3 dependence of $\langle \bar{d}_+(d_3) \rangle$. If the system has a hierarchy of distances, $\bar{d}_+(d_3)$ will have step-like increasing points as d_3 increases, at which d_3 becomes equal to one of them. Even after the sample average, $\langle \bar{d}_+(d_3) \rangle$ for $N = 200$ shows such behaviour at $d_3 \sim 10$, while it is not clear for $N = 100$. When d_3 becomes the largest distance of the hierarchy, $\langle \bar{d}_+(d_3) \rangle$ ceases to increase. This takes place at $d_3 \sim \langle \bar{d} \rangle$, where $W(d_3)$ is quite small. $W(d_3)$ takes the largest value of order 0.1 at $d_3 = 0$. As d_3 increases, $W(d_3)$ for $N = 100$ decreases more rapidly than for

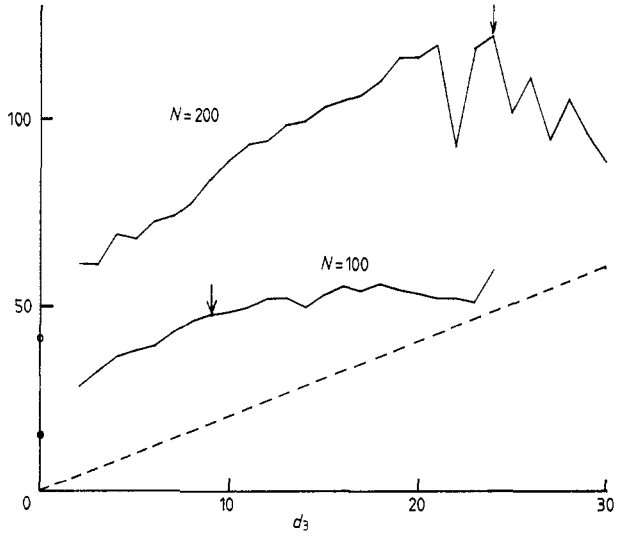

Figure 7. The d_3 dependence of $\langle \bar{d}_+(d_3) \rangle$ at $T = 0.3$. $\langle \bar{d} \rangle$ is marked by arrows for each N. The circles on the vertical axis indicate the values $\langle \bar{d}_+(0) \rangle$ which are 15.04 for $N = 100$ and 40.79 for $N = 200$. The broken line is $2d_3$, which is the lower bound of $\langle \bar{d}_+(d_3) \rangle$.

$N = 200$. This point is expressed by the averages given by

$$\langle \bar{d}_+ \rangle = \left\langle \sum_{d_3=0}^{N/2} \bar{d}_+(d_3)\, W(d_3) \right\rangle \tag{15}$$

$$\langle \bar{d}_- \rangle = \left\langle \sum_{d_3=0}^{N/2} \bar{d}_-(d_3)\, W(d_3) \right\rangle \tag{16}$$

and $\langle \bar{d}_3 \rangle$. At $T = 0.3$ we found $\langle \bar{d}_- \rangle = 0.4967$, $\langle \bar{d}_3 \rangle = 1.2057$ and $\langle \bar{d}_+ \rangle = 18.102$ for $N = 100$, and 1.7191, 5.3170, 55.0867 for $N = 200$. The N dependence of $\langle \bar{d}_+ \rangle$ is related to the dependence of $\langle \bar{d} \rangle$, if there is the typical largest distance which characterises them for each sample. This implies the relation $\langle \bar{d}_+ \rangle \sim 2\langle \bar{d} \rangle$, which is well satisfied for both system sizes. Unfortunately, $\langle \bar{d}_3 \rangle$ does not seem to be proportional to N. The system size $N = 100$ may be still too small to see the hierarchical structure at $T = 0.3$, since the averaged distance $\langle \bar{d} \rangle$ is quite small (~ 9).

4. Discussion

In this section we want to present some discussions on the results and some comments on the short-range model. Our numerical results are qualitatively in good agreement with the results obtained by the replica symmetry breaking theory. In addition to this, our approach leads us to a natural explanation of the ultrametricity of local minima, and also implies the relation $d_1 - d_2 \sim \sqrt{d_3}$ for three distances $d_1 \geqslant d_2 \geqslant d_3$. This relation was not recognised by the $N = \infty$ mean-field theory. In § 3, we checked this relation by a numerical study, which strongly supports the descriptions of local minima presented in § 2. It will be interesting to see if this relation works in studying the fluctuations around the Parisi solution.

We started our study with the observation of $P(h)$, which led us to a heuristic method of obtaining many low-energy local minima. Although our method is suggestive, we have no idea about the mechanism which chooses a few R_h from many possible subgroups of S_h. This aspect may be closely related to the nature of the glassy state, which is definitely distinguished from the paramagnetic state. By the observation in § 2, ultrametricity is reduced to the following statements. (i) There is a sequence of clusters of spins $S_1 \subset S_2 \subset \ldots \subset S_L$ for any low-energy local minimum and, for each S_i, another local minimum is obtained by simultaneously flipping half of the spins R_i in S_i. (ii) The spin flips in each S_i are independent of i. In general, $S_j (j < i)$ will be changed with constraint $S_j \subset S_i$ under the spin flips in S_i. This picture is in agreement with the stochastic branching process derived from the Parisi solution [8]. A very interesting question is whether or not ultrametricity is realised in other random systems, in particular in the short-range model. The numerical study of the three-dimensional $\pm J$ model has been already performed [8]. We here tentatively propose one possibility which satisfies the above two conditions. First of all it should be noticed that, in the short-range model, large clusters whose simultaneous spin flips cost energy of order one should be in unusual geometrical concepts, since the simultaneous flips of spins in a cube or a sphere will cost energy proportional to its surface when the system is renormalised into a low temperature region [13, 14]. Let us imagine two spin clusters, S_1 and S_2 with $S_1 \subset S_2$, for a given local minimum of the short-range model. In figure 8 these clusters are represented by the regions enclosed by broken lines. In each S_i, we introduce another region R_i enclosed by zigzag lines (boundary) in which

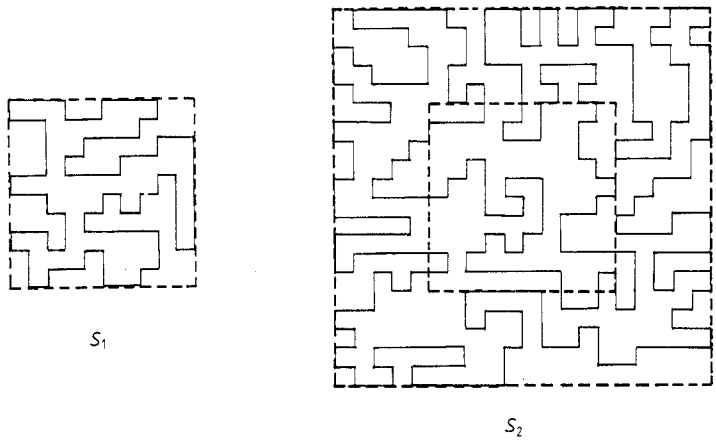

Figure 8. The diagram which explains the possible ultrametricity of the short-range model. The small square enclosed by the broken line is S_1. The large square is S_2. The relation $S_1 \subset S_2$ is shown in the figure on the right. R_i is enclosed by a zigzag line.

simultaneous spin flips take place to another local minimum of nearly the same energy. We should note here that, if the surface of R_i is random enough, the existence of such clusters will not contradict the fact that the system is renormalised into a low-temperature region. In other words, the system can be solid with the simultaneous spin flips in almost all regions, while it is soft with the simultaneous spin flips in a few privileged regions. Then (i) is satisfied if $|R_i| = |S_i|/2$, and (ii) is satisfied if two zigzag lines have no correlation. R_i in figure 8 is obtained by coin tosses on the square lattice on S_i, with suitable rearrangements to ensure the connectivity of R_i and $\bar{R}_i$. In this suggestion, however, we have introduced a serious assumption that the system is not homogeneous but has certain regions in which simultaneous spin flips take place with an energy cost of order one. In this respect we remember that, by the arguments of the renormalisation group transformation, some authors suggest that the short-range model is quite different from the SK model in the properties of overlap functions [15, 16]. However, it is not clear if the usual method in statistical physics works well enough to study such a few privileged clusters of unusual shape. If we stick to the idea presented in this paper, the study of the model with high enough dimension will be illuminating since, in high connectivity, sites of small effective field have a tendency to form a cluster.

Acknowledgments

The author is grateful to Dr K Nemoto, Professor H Takayama and Professor T Tsuneto for discussions on this method.

References

[1] Parisi G 1980 *J. Phys. A: Math. Gen.* **13** L115, 1101, 1887
[2] Sherrington D and Kirkpatrick S 1975 *Phys. Rev. Lett.* **35** 1792
[3] Mézard M, Parisi G, Sourlas N, Toulouse G and Virasoro M 1984 *J. Physique* **45** 843

[4] Parisi G 1983 *Phys. Rev. Lett.* **50** 1946
[5] Parga N and Parisi G 1984 *J. Physique* **45** L1063
[6] Bhatt R N and Young A P 1986 *J. Magn. Maget. Mater.* **54–57** 191
[7] Nemoto K and Takayama H 1986 *J. Magn. Magnet. Mater.* **54–57** 135
[8] Rammal R, Toulouse G and Virasoro M 1986 *Rev. Mod. Phys.* **58** 765
[9] Nokura K 1987 *Prog. Theor. Phys.* **78** 5
[10] Nokura K 1987 *J. Phys. A: Math. Gen.* **20** L1203
[11] Anderson P W 1978 *Ill Condensed Matter, Les Houches 1978* (Amsterdam: North-Holland)
Thouless D J, Anderson P W and Palmer R 1977 *Phil. Mag.* **35** 593
[12] Kirkpatrick S and Sherrington D 1978 *Phys. Rev.* B **17** 4384
[13] McMillan W L 1985 *Phys. Rev.* B **31** 340
[14] Bray A and Moore M A 1985 *Phys. Rev.* B **31** 631
[15] Moore M A and Bray A J 1985 *J. Phys. C: Solid State Phys.* **18** L699
[16] Fisher D S and Huse D A 1987 *J. Phys. A: Math. Gen.* **20** L1005